JOC Article
pubs.acs.org/joc

Mechanism and Regioselectivity of the Osmium-Catalyzed Aminohydroxylation of Olefins

Dominik Munz and Thomas Strassner*

Physikalische Organische Chemie, Technische Universität Dresden, Mommsenstrasse 13, 01062 Dresden, Germany

thomas.strassner@chemie.tu-dresden.de

Received November 12, 2009

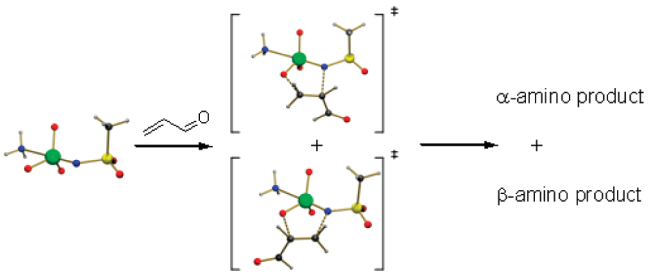

The mechanism and regioselectivity of the osmium-catalyzed aminohydroxylation of olefins was investigated in detail by density functional theory (B3LYP/6-31G(d)) calculations in the gas phase and with the CPCM-solvent model. A systematic variation of the catalyst system (OsO_4 and various nitrogen sources) and the substrate's electronic situation was conducted. Activation barriers could be correlated to Hammett values and linear Gibbs free energy relations could be determined. Experimental results, which indicated an electronic influence on the regioselectivity, could be confirmed and appear to be predictable. The reaction follows a [3+2] mechanism. We additionally report results on the experimentally observed competing dihydroxylation reaction and the ligand-induced reaction rate acceleration.

Introduction

Sharpless et al. reported in the 1970s an aza-analogon of the osmium-catalyzed *cis*-vicinal dihydroxylation (DH)[1] of alkenes, the aminohydroxylation (AH).[2,3] In 1996 it was rendered asymmetric[4] and extended to a large variety of substrates in the following. The AH is synthetically important as it provides straightforward access to the aminoalcohol fragment present in a broad variety of natural products[5,6] and has been extensively reviewed.[7−14] The reaction is usually carried out in alcohol/water solvent mixtures as shown in Scheme 1. The chiral ligand is often derived from the *Cinchona* alkaloids and the catalytically active species is formed in situ from an osmium(VI) salt like $K_2OsO_2(OH)_4$ and a stoichiometric nitrogen source like Chloramine-M. Frequently used nitrogen sources are sulfonamide,[8] carbamate,[1] amide,[1] or *tert*-butyl[2,15] compounds. Generally different regio- and stereoisomers can be formed.

By the right choice of ligands it often seems to be possible to tune the **enantio**selectivity, but the setting of a particular

*To whom correspondence should be addressed. Tel.: +49 351 46338571. Fax: +49 351 46339679.

(1) Kolb, H. C.; VanNieuwenhze, M. S.; Sharpless, K. B. *Chem. Rev.* **1994**, *94*, 2483–2547.
(2) Sharpless, K. B.; Patrick, D. W.; Truesdale, L. K.; Biller, S. A. *J. Am. Chem. Soc.* **1975**, *97*, 2305–2307.
(3) Sharpless, K. B.; Chong, A. O.; Oshima, K. *J. Org. Chem.* **1976**, *41*, 177–179.
(4) Li, G.; Chang, H.-T.; Sharpless, K. B. *Angew. Chem., Int. Ed.* **1996**, *35*, 451–454.
(5) Bergmeier, S. C. *Tetrahedron* **2000**, *56*, 2561–2576.
(6) Li, G.; Sharpless, K. B. *Acta Chem. Scand.* **1996**, *50*, 649–651.
(7) Bodkin, J. A.; McLeod, M. D. *J. Chem. Soc., Perkin Trans. 1* **2002**, 2733–2746.
(8) Kolb, H. C.; Sharpless, K. B. *Transition Metals for Organic Synthesis*, 2nd ed.; Wiley-VCH Verlag GmbH & Co. KGaA: Weinheim, Germany, 2004; Vol. 2, pp 309−326.
(9) Muniz, K. *Chem. Soc. Rev.* **2004**, *33*, 166–174.
(10) O'Brien, P. *Angew. Chem., Int. Ed.* **1999**, *38*, 326–329.
(11) Bolm, C.; Hildebrand, J. P.; Muniz, K. *Catalytic Asymmetric Synthesis*, 2nd ed.; Wiley-VCH: New York, 2000; pp 399−428.
(12) Bayer, A. *Compr. Asymmetric Catal., Suppl.* **2004**, *2*, 43–71.
(13) Nilov, D.; Reiser, O. *Adv. Synth. Catal.* **2002**, *344*, 1169–1173.
(14) Lohray, B. B.; Bhushan, V.; Reddy, G. J.; Reddy, A. S. *Indian J. Chem., Sect. B: Org. Chem. Incl. Med. Chem.* **2002**, *41B*, 161–168.
(15) Rubinstein, H.; Svendsen, J. S. *Acta Chem. Scand.* **1994**, *48*, 439–444.

DOI: 10.1021/jo902421n Published on Web 02/03/2010

SCHEME 1. Aminohydroxylation Reaction with the Oxidans Chloramine-M (H_3CSO_2NCl Na)

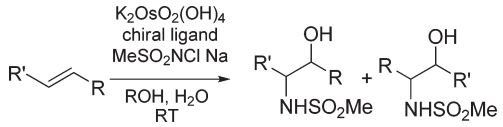

regioselectivity remains challenging,[16] as it is controlled by multiple factors. Steric and electronic contributions of the ligand,[17,18] substrate,[8,18−21] and hydrophobic effects due to the solvent[19] have been experimentally observed and investigated. Janda et al. have proposed a substrate-based methodology[18] to explain the factors controlling the regioselectivity. These are often mutually dependent on each other and experimentally hard to determine, but can be calculated by quantum-chemical calculations.

This work for the first time systematically addresses the electronic influence of substituents R on the $O_3OsN{=}R$ unit as well as of the reacting olefin on the regiochemistry of the AH. As the ligands in general are too big to be calculated by high-level DFT calculations we used model systems to evaluate the different factors which might influence the regioselectivity of the reaction.

Computational Details

All calculations were performed with Gaussian-03,[22] using the density functional/Hartree−Fock hybrid model Becke3LYP[23−26] and the split valence double-ζ (DZ) basis set 6-31G(d)[27] for C, H, O, and S. The Hay−Wadt[28] effective core potential (ECP) was used for osmium, as it has been successfully employed in former studies on the respective dihydroxylation[29] and diamination[30] reaction. No symmetry or internal coordinate constraints were applied during optimizations. All reported ground state structures were verified as being true minima by the absence of negative eigenvalues in the vibrational analysis. Transition state (ts) structures were located with use of the Berny algorithm[31] and it was verified that the Hessian matrix has only one imaginary eigenvalue. The identities of all transition states were confirmed by animating the negative eigenvector coordinate with MOLDEN[32] and intrinsic reaction coordinate (IRC) calculations. Approximate Gibbs free energies (ΔG) and enthalpies (ΔH) were obtained via thermochemical analysis of frequency calculations. This takes into account zero-point effects, thermal enthalpy, and entropy corrections. All energies reported are Gibbs free energies or enthalpies at 298 K, using unscaled frequencies. Atomic partial charges were predicted with the NPA model.[33] Solvation corrections were applied with use of the CPCM-model[34−36] as implemented in Gaussian-03 and we found that the calculated selectivities exhibited a dependence on solvation parameters. After a thorough screening of different solvation parameters in optimizations, single points of the experimental permittivity ε of a 1:1 *tert*-butanol:water mixture (ε = 37.8 F/m ; ε_{inf} = 2.69 F/m) were performed on optimized structures.[37] This solvent mixture is most commonly used in AH reactions.[7] A solvent's mean molecular radius of 2.16 Å, a numerical density of 0.012 $Å^{-3}$ derived by the experimental density,[37] and UAKS cavities[38,39] were utilized. This approach of determining a solvent's radius was recently used by Goddard et al.[40] and does in our opinion reproduce the experimental conditions best. It is described in detail in the Supporting Information. ΔG_{CPCM} corresponds to the addition of rotational and zero-point corrected vibrational energies in the gas phase at 298 K to the electronic energy in solution (ΔE_{CPCM}) as we could not optimize all structures in solvent calculations. The neglect of vibrational and entropic corrections to the gas phase energy seems to be justified as test calculations on selected transition states revealed an error of less than 1 kcal mol^{-1}.

Results and Discussion

To calculate the electronic effects of the nitrogen source and the substrate on the regioselectivity of the AH, it is necessary to first discuss the underlying mechanism ([3+2] or [2+2]) of the AH (**peri**selectivity). We also need to calculate competing reaction pathways, which raises the question of amino- versus dihydroxylation (**chemo**selectivity). The ligand introduces additional questions: Does the reaction proceed by *syn* or *anti* addition? Can we observe a ligand-induced acceleration? Contrary to the DH we also have to address the question of the regioselectivity (α/β) of the AH if the substrate carries different substituents. As electron-donating or -withdrawing substituents at the nitrogen source have been experimentally shown to have an influence on the regiochemistry,[8] also different substituents at the nitrogen source have been investigated.

First we would like to discuss the concerted [3+2] cycloaddition of the olefin to the ligated osmium compound **2** in analogy to the Criegee mechanism[41,42] of the DH (Scheme 2).[18] A competing [3+2] mechanism without ligand coordination via intermediates **3** has to be considered, although it will

(16) Donohoe, T., J.; Chughtai, M. J.; Klauber, D. J.; Griffin, D.; Campbell, A. D. *J. Am. Chem. Soc.* **2006**, *128*, 2514–2515.
(17) Tao, B.; Schlingloff, G.; Sharpless, K. B. *Tetrahedron Lett.* **1998**, *39*, 2507–2510.
(18) Han, H.; Cho, C.-W.; Janda, K. D. *Chem.—Eur. J.* **1999**, *5*, 1565–1569.
(19) Reddy, K. L.; Sharpless, K. B. *J. Am. Chem. Soc.* **1998**, *120*, 1207–1217.
(20) Harding, M.; Bodkin, J. A.; Issa, F.; Hutton, C. A.; Willis, A. C.; McLeod, M. D. *Tetrahedron* **2009**, *65*, 831–843.
(21) Morgan, A. J.; Masse, C. E.; Panek, J. S. *Org. Lett.* **1999**, *1*, 1949–1952.
(22) Frisch, M. J. et al. *Gaussian03*, Rev. E 01; Gaussian Inc.: Wallingford, CT, 2004.
(23) Vosko, S. H.; Wilk, L.; Nusair, M. *Can. J. Phys.* **1980**, *58*, 1200–1211.
(24) Lee, C.; Yang, W.; Parr, R. G. *Phys. Rev. B: Condens. Matter Mater. Phys.* **1988**, *37*, 785–789.
(25) Becke, A. D. *J. Chem. Phys.* **1993**, *98*, 5648–5652.
(26) Stephens, P. J.; Devlin, F. J.; Chabalowski, C. F.; Frisch, M. J. *J. Phys. Chem.* **1994**, *98*, 11623–11627.
(27) Hehre, W. J.; Ditchfield, R.; Pople, J. A. *J. Chem. Phys.* **1972**, *56*, 2257–2261.
(28) Hay, P. J.; Wadt, W. R. *J. Chem. Phys.* **1985**, *82*, 299–310.
(29) DelMonte, A. J.; Haller, J.; Houk, K. N.; Sharpless, K. B.; Singleton, D. A.; Strassner, T.; Thomas, A. A. *J. Am. Chem. Soc.* **1997**, *119*, 9907–9908.
(30) Deubel, D. V.; Muniz, K. *Chem.—Eur. J.* **2004**, *10*, 2475–2486.
(31) Schlegel, H. B. *J. Comput. Chem.* **1982**, *3*, 214–218.
(32) Schaftenaar, G.; Noordik, J. H. *J. Comput.-Aided Mol. Des.* **2000**, *14*, 123–134.
(33) Reed, A. E.; Curtiss, L. A.; Weinhold, F. *Chem. Rev.* **1988**, *88*, 899–926.
(34) Barone, V.; Cossi, M. *J. Phys. Chem. A* **1998**, *102*, 1995–2001.
(35) Miertus, S.; Scrocco, E.; Tomasi, J. *Chem. Phys.* **1981**, *55*, 117–129.
(36) Klamt, A.; Schueuermann, G. *J. Chem. Soc., Perkin Trans. 2* **1993**, 799–805.
(37) Tabellout, M.; Lanceleur, P.; Emery, J. R.; Hayward, D.; Pethrick, R. A. *J. Chem. Soc., Faraday Trans.* **1990**, *86*, 1493–1501.
(38) Barone, V.; Cossi, M.; Tomasi, J. *J. Chem. Phys.* **1997**, *107*, 3210–3221.
(39) McLean, A. D.; Chandler, G. S. *J. Chem. Phys.* **1980**, *72*, 5639–5648.
(40) Xu, X.; Kua, J.; Periana, R. A.; Goddard, W. A. III *Organometallics* **2003**, *22*, 2057–2068.
(41) Criegee, R. *Justus Liebigs Ann. Chem.* **1936**, *522*, 75–96.
(42) Torrent, M.; Deng, L.; Duran, M.; Sola, M.; Ziegler, T. *Organometallics* **1997**, *16*, 13–19.
(43) Only the most stable regioisomeres are shown in Schemes 2 and 3.

SCHEME 2. [3+2] Mechanism of the Aminohydroxylation (AH) and Dihydroxylation (DH)[43]

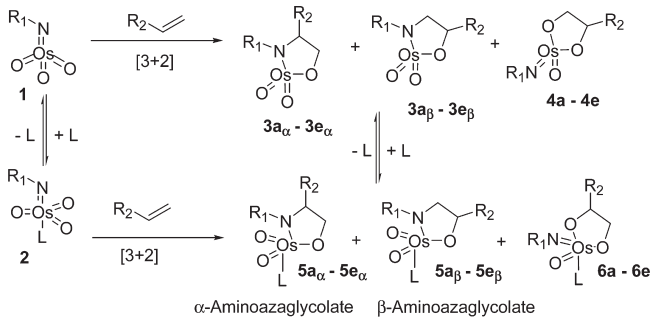

R_1 = -SO_2Me (**mes_**), -$SO_2{}^p$Tol (**tos_**), -CN (**cn_**) , -H (**h_**), -Me (**me_**)
R_2 = -H (**a**), -CHO (**b**), -Me (**c**), -C_2H_3 (**d**), -CN (**e**)
L = nitrogen ligand

almost certainly lead to the experimental observation of a lower overall enantioselectivity, as no chiral ligand is involved in the rate-determining reaction step (Scheme 2). In every case two different regioisomers may result: the α-amino $\mathbf{5}_\alpha$ and the *β*-amino products $\mathbf{5}_\beta$. Those are being hydrolyzed consecutively in situ to yield the aminoalcohol. Furthermore competing dihydroxylation mechanisms leading to **6** had to be considered.

We chose the substituents R_1 on the imido nitrogen atom and R_2 on the olefin due to their assigned Hammett substituent parameters.[44,45] R_1 defines mesyl (**mes_**), tosyl (**tos_**), hydrogen (**h_**), cyano (**cn_**), or methyl (**me_**) substituents, R_2 different substrates, which are ethylene (**a**), acrolein (**b**), propene (**c**), butadiene (**d**), and acrylonitrile (**e**).

To model the electronic effect of the coordination of the chiral nitrogen ligand L, ammonia has been chosen. This simplification (with precedence in the literature)[29,46−48] was necessary considering the number of calculated structures and the size of the large cinchona-derived ligands. Test calculations with the ligand NMe_3 showed only minor energy differences of less than 0.5 kcal mol^{-1} compared to those of ammonia.

According to the original proposal the reaction could also follow a formal [2+2] cycloaddition of the alkene to give the osmaazetidin intermediate **7a**, which might rearrange under coordination of the nitrogen ligand L to the osmium azaglycolate **5a** (Scheme 3)[49] and the osmaoxetane intermediate **8a**, which can rearrange either to **5a** or the DH product **6a**. Moreover a [2+2] cycloaddition of ethylene to compound **2** might yield **9a** (which could rearrange to **5a**) as well as **10a** (which could rearrange to afford **5a** or **6a**).

SCHEME 3. [2+2] Mechanism of the Aminohydroxylation (AH) and Dihydroxylation (DH)

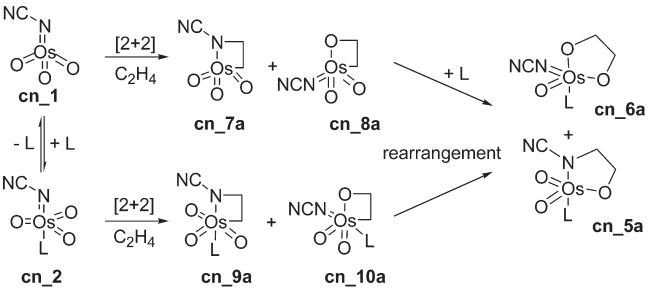

For the DH isotope effect studies and quantum-chemical calculations revealed a significant preference for the [3+2] mechanism,[29,42,50−54] which is also the favored mechanism in the case of the Os(VIII)-catalyzed diamination.[30] However, investigations on complexes of the general type LMO_3 (where L could also be oxygen) indicated that the activation barriers strongly depend on the ligand L and the transition metal M, which might even lead to a situation where a [2+2] mechanism is favored.[53,55,56] It was also shown that the activation barriers for the [3+2] cycloaddition of ethylene to LMO_3 type complexes can be predicted according to the Marcus theory.[57] We therefore did not expect the reaction to proceed via a [2+2] mechanism and checked only for one case, the reaction of the nitrile-substituted imidotrioxoosmium complex with ethylene.

Peri- and Chemoselectivity. We calculated the aminohydroxylation transition states for the [3+2] cycloadditions of ethylene to the cyano-substituted imidotrioxoosmium complexes **cn_1** (leading to **cn_3a**) and **cn_2** (with L = NH_3, leading to **cn_5a**) (Scheme 2) and compared them to the [2+2] reaction pathway. Additions across the Os=N bond lead to the osmaazetidine intermediates **cn_7a** and **cn_9a**, whereas addition across the Os=O bond affords the osmaoxetanes **cn_8a** and **cn_10a**, which could rearrange to **cn_5a** and **cn_6a** (Scheme 3). Table 1 gives enthalpies and Gibbs free energies of transition states and products with the ammonia ligand in the *anti*-position relative to the imido group.

The [2+2] cycloadditions (entries 1−4) are kinetically and thermodynamically disfavored by more than 25 kcal mol^{-1} compared to the [3+2] mechanism (entries 5 and 6). Although we only checked one example, we can expect that also for the substituted olefins the [2+2] reaction pathway is not favored.

For the cycloaddition step of the [3+2] addition a ligand-induced reaction-rate acceleration of 2.7 kcal mol^{-1} was calculated. The coordination of the model ligand NH_3 leads (in agreement with Hammond's postulate) to shorter O−C (2.277 vs 2.301 Å) and N−C (2.397 vs 2.455 Å) distances in the transition state (Chart 1).

To study the chemoselectivity (DH versus AH) we investigated the effect of the five electronically different substituents R_1 (Scheme 2), but restricted the variety of alkenes to

(44) Hammett, L. P. *J. Am. Chem. Soc.* **1937**, *59*, 96–103.
(45) Hansch, C.; Leo, A.; Taft, R. W. *Chem. Rev.* **1991**, *91*, 165–195.
(46) Ess, D. H. *J. Org. Chem.* **2009**, *74*, 1498–1508.
(47) Ujaque, G.; Maseras, F.; Lledos, A. *Eur. J. Org. Chem.* **2003**, 833–839.
(48) Strassner, T.; Drees, M. *THEOCHEM* **2004**, *671*, 197–204.
(49) Sharpless, K. B.; Teranishi, A. Y.; Backvall, J. E. *J. Am. Chem. Soc.* **1977**, *99*, 3120–3128.
(50) Dapprich, S.; Ujaque, G.; Maseras, F.; Lledos, A.; Musaev, D. G.; Morokuma, K. *J. Am. Chem. Soc.* **1996**, *118*, 11660–11661.
(51) Pidun, U.; Boehme, C.; Frenking, G. *Angew. Chem., Int. Ed.* **1997**, *35*, 2817–2820.
(52) Deubel, D. V.; Frenking, G. *J. Am. Chem. Soc.* **1999**, *121*, 2021–2031.
(53) Deubel, D. V.; Schlecht, S.; Frenking, G. *J. Am. Chem. Soc.* **2001**, *123*, 10085–10094.
(54) Deubel, D. V. *Angew. Chem., Int. Ed.* **2003**, *42*, 1974–1977.
(55) Chen, X.; Zhang, X.; Chen, P. *Angew. Chem., Int. Ed.* **2003**, *42*, 3798–3801.
(56) Pietsch, M. A.; Russo, T. V.; Murphy, R. B.; Martin, R. L.; Rappe, A. K. *Organometallics* **1998**, *17*, 2716–2719.
(57) Gisdakis, P.; Roesch, N. *J. Am. Chem. Soc.* **2001**, *123*, 697–701.

TABLE 1. Periselectivity: Activation ($\Delta H^{\ddagger}$) and Reaction Enthalpies (ΔH) as well as Gibbs Free Energies ($\Delta G^{\ddagger}$ and ΔG) of cn_1/cn_2 with Ethylene in Solvent (in kcal mol^{-1} at 298.15 K)[a]

entry	reaction	$\Delta H^{\ddagger}_{CPCM}$ ($\Delta H^{\ddagger}$)	$\Delta G^{\ddagger}_{CPCM}$ ($\Delta G^{\ddagger}$)	ΔH_{CPCM} (ΔH)	ΔG_{CPCM} (ΔG)
1	**cn_1 → cn_7a**	37.7 (42.4)	52.2 (56.8)	28.8 (35.5)	42.9 (49.6)
2	**cn_1 → cn_8a**	32.3 (32.9)	45,9 (46,6)	−5.0 (−3.8)	9,2 (10.4)
3	**cn_2 → cn_9a**	29.2 (37.5)	44.7 (53.0)	28.3 (33.5)	43.8 (51.1)
4	**cn_2 → cn_10a**	27.8 (40.2)	41.9 (54.3)	1.2 (4.6)	15.6 (18.9)
5	**cn_1 → cn_3a**	2.0 (0.8)	15.2 (14.0)	−53.7 (−49.1)	−38.7 (−34.1)
6	**cn_2 → cn_5a**	−0.2 (−0.1)	12.5 (12.7)	−62.1 (−55.6)	−46.6 (−40.2)

[a]Gas phase results are given in parentheses.

CHART 1. [3+2] Transition States for the Reaction of OsO_3NCN and $OsO_3(NH_3)NCN$ with Ethylene[a]

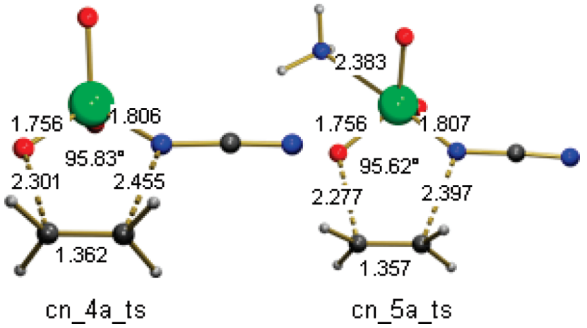

[a]Bond lengths are given in Å, angles in deg.

SCHEME 4. *Anti*- and *Syn*-Addition of the Nitrogen Ligand

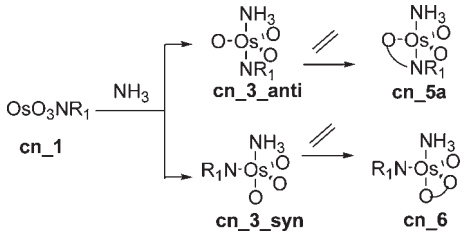

ethylene. In all DH cases the *syn*-[3+2] transition states (e.g., leading to **cn_6**, Scheme 4) turned out to be favored, whereas for the AH transition states an *anti*-alignment of the NH_3 group with respect to the imido group is lower in energy (e.g., leading to **cn_5a**, Scheme 4). Additional data can be found in the Supporting Information.

Gibbs free reaction energies for the *anti*-addition (**1** + NH_3 → **2**, Scheme 2) of ammonia to the five different trioxoimidoosmium compounds **1** is summarized in Figure 1. It is exergonic for strongly electron withdrawing substituents (OsO_3NCN: −3.5 kcal mol^{-1}) and endergonic in the case of methyl or hydrogen substituents (OsO_3NH: 3.3 kcal mol^{-1}; OsO_3NMe: 4.1 kcal mol^{-1}). *Syn*-addition is less favorable; the results are given in the Supporting Information.

As the reaction involves the coordination of the amine ligand and the formation of the product as shown in Scheme 5, both steps have to be considered in order to predict the overall reaction rate acceleration effects for the different substituents R_1 (Table 2). According to the Curtin−Hammett principle only $\Delta\Delta G^{\ddagger}$ is decisive for the overall selectivity of competing reactions.

(58) Transition states **mes_5a_ts** like **mes_5c$_\beta$_ts** in Figures 2, 3, 5 were obtained due to convergence of forces.

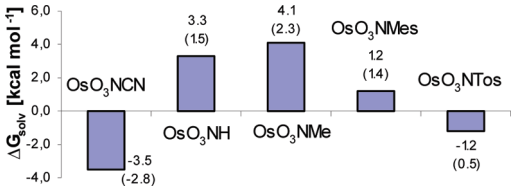

FIGURE 1. Gibbs free reaction energies ΔG of the *anti*-addition **1** + NH_3 → **2** (in kcal mol^{-1}). Gas phase results are given in parentheses.

SCHEME 5. Ammonia Ligand Addition and Effects on Overall Selectivity

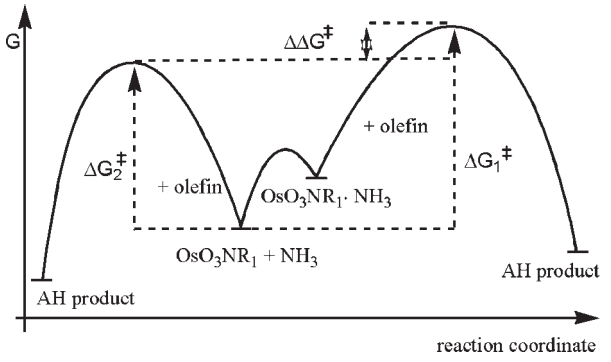

Table 2 gives the calculated activation barriers leading either to the DH or AH products. In all cases the DH was calculated to be higher in activation energy compared to the AH. Except in the case of the hydrogen substituent (entry 2) a ligand-induced reaction rate accelerating effect of the AH was predicted. The major difference between the DH and AH transition states is the preferred orientation of the nitrogen ligand which in the case of the DH prefers to be *syn* while for the AH transition states the *anti*-position of the ligand is preferred.

Regioselectivity. To analyze the effect of the different substituents R_1 (Scheme 2) as well as the electronic effects of the alkene substituents R_2 (Scheme 2) we calculated all [3+2] transition states leading to the **5α**- and **5*β***-regioisomers. All calculated structures, their energies, and coordinates are given in the Supporting Information. The results for the regioselectivity of the [3+2] addition are summarized in Figure 2. The calculated β-selectivity is given by the difference $\Delta G^{\ddagger}_{\alpha} - \Delta G^{\ddagger}_{\beta}$.

The β-addition is predicted to be preferred not only kinetically, but also thermodynamically. The Hammett plots for the nitrile (**cn_**) and sulfonamide (**mes**/**tos_**) substituents are given in Figure 3. The substituents R_1 (Scheme 2) have been chosen by their Hammett parameters to reflect the experimentally used substituents. From the

TABLE 2. Activation Energies $\Delta G^{\neq}$ for the [3+2] Additions of OsO_3N-R_1 to Ethylene According to Scheme 5 (in kcal mol^{-1})[a] [58]

					
Entry	Substituent	$\Delta G_1^{\neq}$	$\Delta G_2^{\neq}$	$\Delta G_1^{\neq}$	$\Delta G_2^{\neq}$
1	R_1 = CN	9.1 (9.9)	15.2 (14.0)	13.1 (13.9)	15.9 (15.2)
2	R_1 = H	16.9 (14.4)	14.0 (13.2)	23.3 (22.7)	20.8 (19.4)
3	R_1 = Me	19.9 (17.6)	21.0 (19.7)	28.2 (25.4)	21.6 (19.7)
4	R_1 = mesyl	12.8 (12.3)	15.1 (13.6)	15.0 (14.5)	15.2 (14.5)
5	R_1 = tosyl	11.8 (12.8)	14.0 (13.4)	15.0 (15.3)	14.3 (14.6)

[a]Gas phase results are given in parentheses.

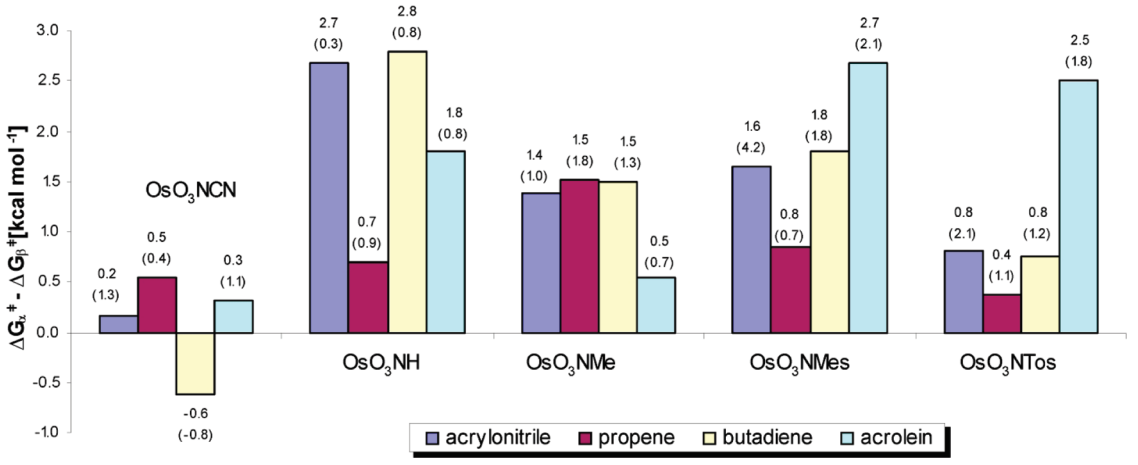

FIGURE 2. [3+2] β-addition is preferred over the α-addition (in kcal mol^{-1}). Gas phase results are given in parentheses.[58]

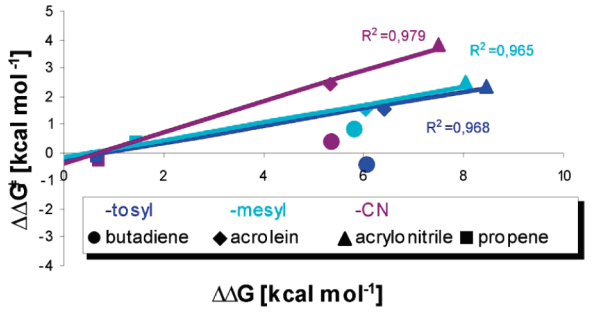

FIGURE 3. Hammett plot of the β-addition of the nitrile (**cn_**), tosyl (**tos_**), and mesyl (**mes_**) systems.

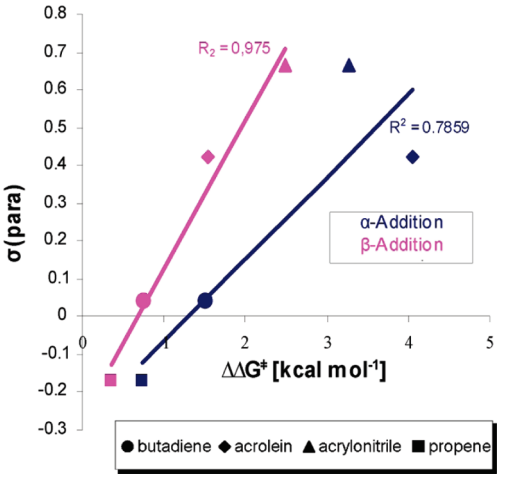

FIGURE 4. Correlation between the activation barriers of the [3+2] transition states **tos_5a$_\alpha$-tos_5e$_\alpha$** and **tos_5a$_\beta$-tos_5e$_\beta$** to tabulated *p*-Hammett constants of the alkenes.

calculated results it can be predicted that substituents with higher Hammett constants will lead to higher activation energies.

The Hammett plots ($\Delta\Delta G$ is given relative to ethylene) show a large deviation for butadiene, in case of R_1 = CN even the inverse selectivity toward the α-product is predicted (Figure 3). We therefore analyzed the NPA charges of all transition states (given in the Supporting Information) as well as the Kohn−Sham HOMO−LUMO gaps. The amount of net charge transfer from the alkene to the transition metal compound is higher in the case of α-addition than β-addition, whereas the β-addition transition states can be characterized by a larger dipolarity of the double bond of the reacting olefin. The donation of electron density from the alkene to the metal seems to be an important contribution. A similar observation by charge decomposition analysis had been made in the case of the addition to $OsO_2(NH_2)_2$ or OsO_4.[30,54]

The calculated β-selectivity is in agreement with the experimentally observed nitrogen addition to the less substituted carbon atom of the olefin. In the symmetric

CHART 2. Transition States of the CN Substituted System

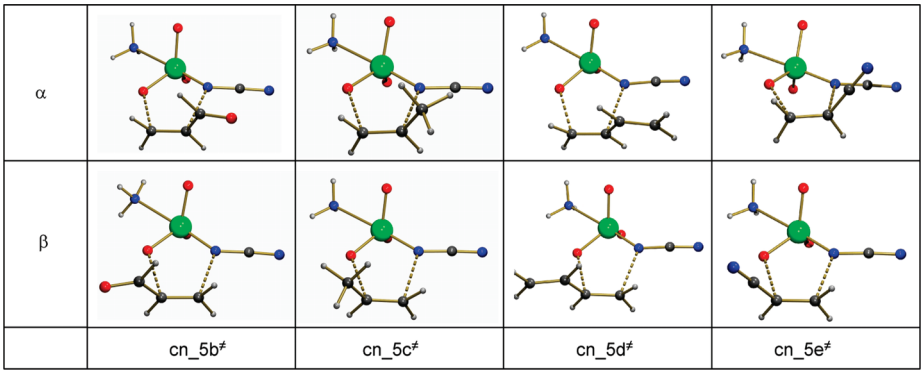

TABLE 3. Calculated Activation Energies and Selected Bond Lengths, Angles, and Dihedrals of the Transition States Shown in Chart 2

transition state	O−Os−N angle (deg)	O−C bond length (Å)	N−C bond length (Å)	C−C bond length (Å)	Os−N−C−C dihedral angle (deg)	$\Delta G^{\ddagger}$ (kcal mol^{-1})
cn_5a_ts	95.8	2.301	2.456	1.357	0.00	12.5
cn_5b$_\alpha$_ts	95.2	2.128	2.423	1.372	2.3	15.3
cn_5b$_\beta$_ts	94.8	2.263	2.309	1.370	1.3	14.9
cn_5c$_\alpha$_ts	94.9	2.253	2.492	1.365	11.6	12.8
cn_5c$_\beta$_ts	95.2	2.329	2.433	1.363	−11.1	12,2
cn_5d$_\alpha$_ts	95.3	2.197	2.581	1.374	11.8	12.3
cn_5d$_\beta$_ts	94.5	2.339	2.345	1.373	−14.6	12.9
cn_5e$_\alpha$_ts	94.4	2.075	2.401	1.378	11.9	16.5
cn_5e$_\beta$_ts	94.3	2.252	2.251	1.375	−5.6	16.4

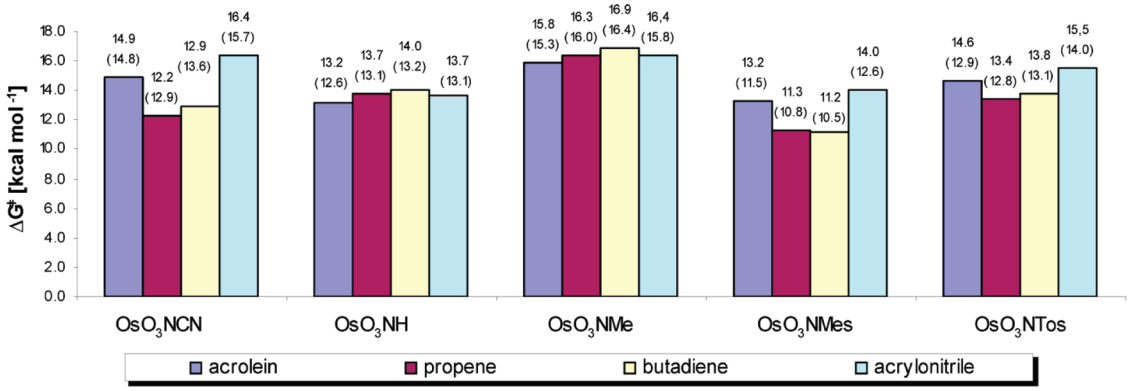

FIGURE 5. Gibbs free energies of activation for [3+2] β-transition states.

aminohydroxylation[3,59] as well as in the asymmetric version, the nitrogen atom usually ends up away from the most electron withdrawing group of the olefin.[8,18,60−62]

This is also in agreement with the experimental observation, that conjugated systems like cyclohexadiene or *E*-1-phenylpropene often show a preference for the α-addition.[3] In the literature this is sometimes also explained by ligand/solvent interactions.[19,62] But as we can correlate activation barriers to tabulated Hammett substituent values of the olefins (e.g., for the tosyl substituent in Figure 4) we propose a relation between electron donating substituents and decreasing preference for β-addition in general. This is nicely demonstrated by the decreasing distance between the linear regression lines for α- and β-addition for small Hammett σ-values (Figure 4).

All α-transition states show more asynchronicity (Chart 2, Table 3) resulting in longer distances to the imido nitrogen atom. We observed the same trend for all systems, but for clarity of the presentation decided to only show the transition states for the cyano system.

Figure 5 compares the Gibbs free energies for the transition states leading to the β-products. The difference of the activation energies of all 20 transition states is relatively small (11.2−16.9 kcal mol^{-1}). The lowest activation energy was calculated for an electron withdrawing substituent (R_1 = mes) and butadiene, an electron rich olefine, the highest for an electron donating substituent (R_1 = me) and butadiene. In general the combination of electron donating substituent and electron rich substrate is unfavorable. But electron withdrawing groups on the alkene as well as on the

(59) Herranz, E.; Sharpless, K. B. *J. Org. Chem.* **1978**, *43*, 2544–2548.
(60) Li, G.; Angert, H. H.; Sharpless, K. B. *Angew. Chem., Int. Ed.* **1997**, *35*, 2813–2817.
(61) Rudolph, J.; Sennhenn, P. C.; Vlaar, C. P.; Sharpless, K. B. *Angew. Chem., Int. Ed.* **1997**, *35*, 2810–2813.
(62) Bruncko, M.; Schlingloff, G.; Sharpless, K. B. *Angew. Chem., Int. Ed.* **1997**, *36*, 1483–1486.

metal also lead to a higher barrier (e.g., R_1 = **cn**; acrylonitrile). The substituent R_1 plays an important role and systems with electron withdrawing groups are predicted to lead to better results than those with electron donating groups (propene, R_1 = **cn** (12.2 kcal mol^{-1}); R_1 = **tos** (13.4 kcal mol^{-1})). Substrates with electron withdrawing groups are predicted to have higher activation barriers. In agreement with the observed higher reactivity, the activation barriers for the mesyl system are predicted to be lower in energy compared to the tosyl nitrogen source.[61] Substituents with high Hammett values[63] seem to be best suited for the aminohydroxylation.

Conclusion

We studied the mechanism and regioselectivity of the osmium-catalyzed aminohydroxylation reaction by density functional theory on the B3LYP/6-31G* level of theory. After confirming that the reaction most likely proceeds by a [3+2] and not by a [2+2] mechanism, we found evidence for a ligand induced acceleration of the reaction rate. Various nitrogen sources with different Hammett parameters are used in the experiments. To model the influence of those substituents we looked at electron withdrawing and donating substituents with similar Hammett values. We studied the effect on the mechanism and the product distribution for the reaction with ethylene. Additionally we used alkenes with different electron withdrawing and donating groups (propene, acrolein, butadiene, acrylonitrile) to study the regiochemistry.

Overall it has been predicted that β-addition is favored. Electron deficient OsO_3N-R complexes are predicted to lead to better results than those with electron donating groups. For olefins with electron withdrawing groups higher activation barriers are predicted and the olefin reactivity could be correlated to their assigned para-Hammett values. The mesyl system is predicted to be the most favorable nitrogen source.

Supporting Information Available: Atomic coordinates of transition and ground states, energies (ΔE, ΔH, ΔG, ΔE_{CPCM}, ΔH_{CPCM}, ΔG_{CPCM}), imaginary frequencies, solvent model details, NPA charges, Kohn−Sham HOMO−LUMO gaps, and complete ref 22. This material is available free of charge via the Internet at http://pubs.acs.org.

(63) *p*-Hammett constants: −Me, −0.17; −H, 0.00, −CN, 0.66; tosyl, 0.68; mesyl, 0.72.